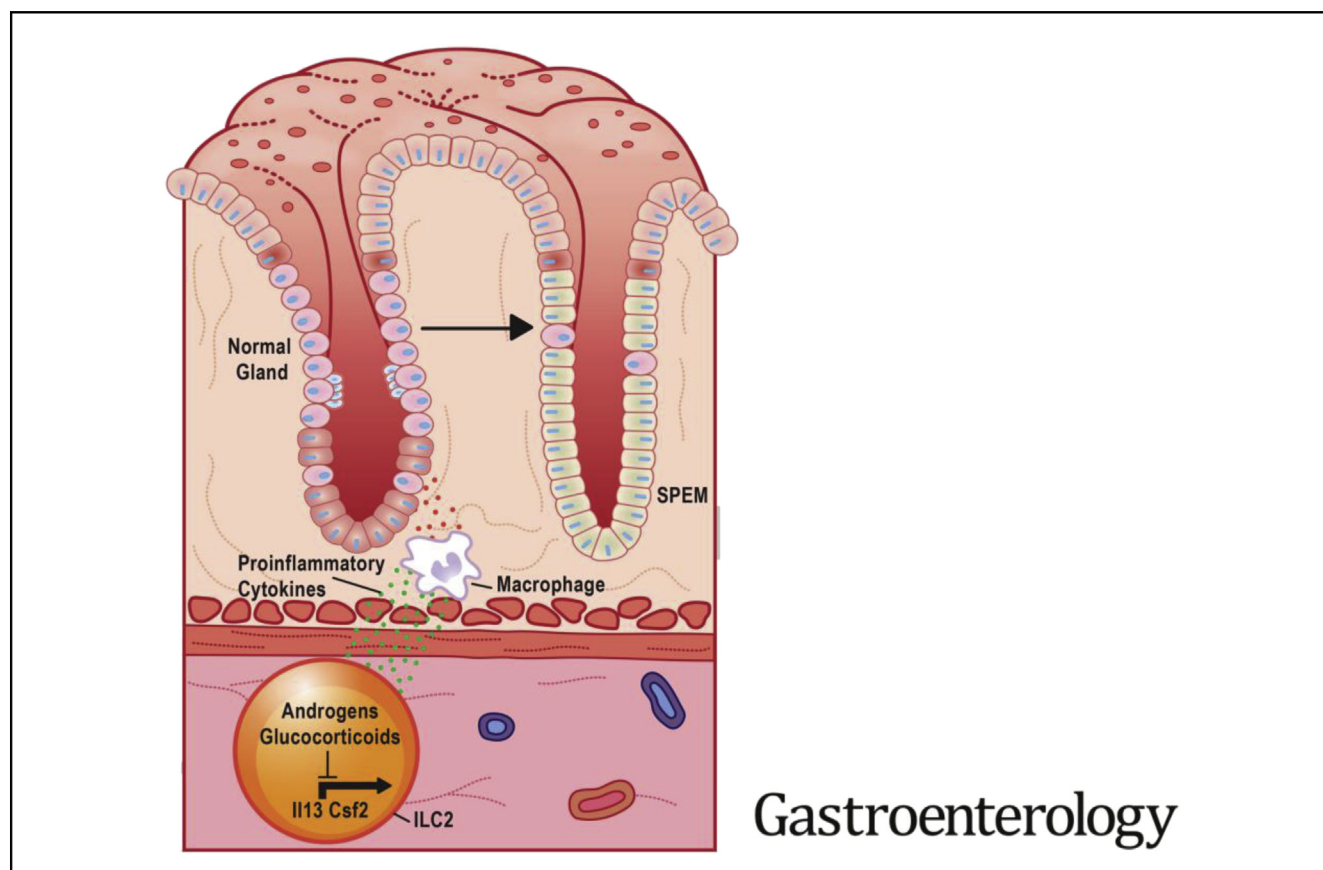


# Glucocorticoids and Androgens Protect From Gastric Metaplasia by Suppressing Group 2 Innate Lymphoid Cell Activation

Jonathan T. Busada,<sup>1,4</sup> Kylie N. Peterson,<sup>1</sup> Stuti Khadka,<sup>4</sup> Xiaojiang Xu,<sup>2</sup> Robert H. Oakley,<sup>1</sup> Donald N. Cook,<sup>3</sup> and John A. Cidlowski<sup>1</sup>

<sup>1</sup>Molecular Endocrinology Group, Signal Transduction Laboratory, <sup>2</sup>Integrative Bioinformatics Support Group, Epigenetics and Stem Cell Biology Laboratory, and <sup>3</sup>Immunogenetics Group, Immunity, Inflammation, and Disease Laboratory, National Institute of Environmental Health Sciences, National Institutes of Health, Research Triangle Park, North Carolina; and <sup>4</sup>Department of Microbiology, Immunology and Cell Biology, West Virginia University School of Medicine, Morgantown, West Virginia



**BACKGROUND & AIMS:** The immune compartment is critical for maintaining tissue homeostasis. A weak immune response increases susceptibility to infection, but immune hyperactivation causes tissue damage, and chronic inflammation may lead to cancer development. In the stomach, inflammation damages the gastric glands and drives the development of potentially preneoplastic metaplasia. Glucocorticoids are potent anti-inflammatory steroid hormones that are required to suppress gastric inflammation and metaplasia. However, these hormones function differently in males and females. Here, we investigate the impact of sex on the regulation of gastric inflammation. **METHODS:** Endogenous glucocorticoids and male sex hormones were removed from mice using adrenalectomy and castration, respectively. Mice were treated with 5 $\alpha$ -dihydrotestosterone (DHT) to test the effects of androgens on regulating gastric inflammation. Single-cell RNA sequencing of gastric leukocytes was used to identify the leukocyte populations that were the direct targets of androgen signaling.

Type 2 innate lymphoid cells (ILC2s) were depleted by treatment with CD90.2 antibodies. **RESULTS:** We show that adrenalectomized female mice develop spontaneous gastric inflammation and spasmolytic polypeptide-expressing metaplasia (SPEM) but that the stomachs of adrenalectomized male mice remain quantitatively normal. Simultaneous depletion of glucocorticoids and sex hormones abolished the male-protective effects and triggered spontaneous pathogenic gastric inflammation and SPEM. Treatment of female mice with DHT prevented gastric inflammation and SPEM development when administered concurrent with adrenalectomy and also reversed the pathology when administered after disease onset. Single-cell RNAseq of gastric leukocytes revealed that ILC2s expressed abundant levels of both the glucocorticoid receptor (*Gr*) and androgen receptor (*Ar*). We demonstrated that DHT treatment potently suppressed the expression of the proinflammatory cytokines *Il13* and *Csf2* by ILC2s. Moreover, ILC2 depletion protected the stomach from SPEM development.

**CONCLUSIONS:** Here, we report a novel mechanism by which glucocorticoids and androgens exert overlapping effects to regulate gastric inflammation. Androgen signaling within ILC2s prevents their pathogenic activation by suppressing the transcription of proinflammatory cytokines. This work revealed a critical role for sex hormones in regulating gastric inflammation and metaplasia.

**Keywords:** Stomach; Gastric; SPEM; Macrophage; ILC2.

The immune system is critical for maintaining tissue homeostasis. Although acute hyperactive inflammation can induce tissue damage, chronic inflammation promotes tissue dysfunction and favors cancer development. Inflammation is regulated differently in males and females due, in part, to the actions of sex steroid hormones.<sup>1,2</sup> Women typically are more resistant than men to infection and mount more robust immune responses to vaccination.<sup>3,4</sup> However, women are also more prone to inflammatory diseases, and 80% of autoimmune diseases occur in women.<sup>5</sup> Similar trends are evident within the stomach, where both *Helicobacter pylori*-independent gastritis and autoimmune gastritis are more common in women.<sup>6</sup> Although men are more resistant to these inflammatory pathologies, some studies report that men are more susceptible to *H. pylori* infection and harbor higher bacterial loads.<sup>7-9</sup> It is clear that sex has a profound role in regulating inflammation; however, the underlying cellular and molecular mechanisms by which sex impacts inflammation are poorly defined.

Within the stomach, immune hyperactivation damages the epithelium and induces the development of spasmolytic polypeptide-expressing metaplasia (SPEM).<sup>10-12</sup> Acute SPEM develops as chief cells transdifferentiate and may function as a healing mechanism.<sup>13,14</sup> However, chronic SPEM is associated with the development of gastric adenocarcinoma.<sup>12,15</sup> Recent studies report that SPEM development is driven by an immune axis of tissue-resident type 2 innate lymphoid cells (ILC2s) and recruited macrophages.<sup>10,11,16</sup> ILC2s are tissue-resident leukocytes that are widely distributed along mucosal surfaces and respond to epithelial stress to initiate inflammation.<sup>17</sup> Activated ILC2s produce large quantities of the cytokines interleukin (IL) 4, IL5, IL13, and colony stimulating factor (CSF) 2 (also known as granulocyte-macrophage CSF).<sup>18-20</sup> These cytokines, in turn, promote the recruitment and activation of monocyte-derived macrophages.<sup>21</sup> Several recent studies have reported that monocyte-derived macrophages damage the gastric epithelium and induce metaplasia development.<sup>10,16,22</sup> The exact mechanisms by which inflammation contributes to SPEM development are poorly defined.

Androgens, the chief male sex hormone, signal through the androgen receptor (AR). Macrophages readily respond to androgens but, although some tissue-specific macrophage populations, such as alveolar macrophages,<sup>23</sup> have been shown to express the AR, it is unclear if macrophages within the gastrointestinal tract express these receptors. Recently, it has become clear that ILC2s are regulated in a sex-specific

## WHAT YOU NEED TO KNOW

### BACKGROUND AND CONTEXT

Inflammation is regulated differently in males and females. Women tend to have higher rates of inflammatory disease than men, including diseases that affect the stomach. The underlying mechanisms by which sex hormones modulate gastric inflammation are unknown.

### NEW FINDINGS

This study reveals a critical role for androgens in regulating gastric inflammation. Androgens signal through type 2 innate lymphoid cells to suppress pathogenic inflammation and metaplasia development.

### LIMITATIONS

These studies were performed in mice. Future studies will assess if similar mechanisms regulate gastric inflammation in humans.

### IMPACT

This study reveals critical mechanisms underlying sex differences in gastric inflammation and inflammatory disease. Clinicians may consider if disrupted glucocorticoid or androgen signaling are contributing factors to gastric inflammatory disease.

manner. Androgens suppress ILC2 proliferation, and male mice have fewer lung ILC2s than females.<sup>24</sup> Male mice are also resistant to IL33-induced asthma due to dampened ILC2 activation. However, castration abolishes these male-protective effects, leading to a significant expansion of lung ILC2s and sensitizing males to asthma. Moreover, prolonged treatment of cultured primary ILC2s with the androgen 5 $\alpha$ -dihydrotestosterone (DHT) suppresses their production of proinflammatory cytokines, including IL13.<sup>25</sup> However, the mechanisms by which androgens signal within ILC2s to regulate proinflammatory gene expression is unknown.

The AR is a ligand-dependent transcription factor. The AR has high homology to the glucocorticoid receptor (NR3C1, hereafter GR), another steroid hormone receptor with potent anti-inflammatory properties.<sup>26,27</sup> We have previously shown that glucocorticoids suppress pathogenic gastric inflammation, and disruption of glucocorticoid signaling induces spontaneous gastric inflammation and metaplasia in female mice.<sup>10</sup> A primary mechanism by which the AR and GR regulate gene transcription is through recognizing specific DNA sequences. The DNA response

**Abbreviations used in this paper:** ADX + CAST, adrenalectomized + castrated; AR, androgen receptor; CSF, colony stimulating factor; DHT, 5 $\alpha$ -dihydrotestosterone; GR, glucocorticoid receptor; GSII, *Griffonia simplicifolia* lectin; IHC, immunohistochemistry; IL, interleukin; ILC2, type 2 innate lymphoid cell; KO, knock-out; mRNA, messenger RNA; NIH, National Institutes of Health; PBS, phosphate-buffered saline; PCR, polymerase chain reaction; RT, reverse transcription; scRNAseq, single-cell RNA sequencing; SPEM, spasmolytic polypeptide expressing metaplasia; UMI, unique molecular identifier.

elements recognized by the AR and GR are nearly identical.<sup>28,29</sup> Indeed, in prostate cancer cells, glucocorticoids can regulate the expression of androgen-dependent genes, providing a route for cancer cells to escape anti-androgen therapies.<sup>30</sup> These results raise the possibility that a similar form of regulation might exist within gastric ILC2s where glucocorticoids and androgens may exert redundancies to suppress proinflammatory gene expression. In this study, we report a novel role for androgens in suppressing gastric inflammation and metaplasia. Moreover, we show that ILC2s co-express the AR and GR and that treatment with either androgens or glucocorticoids can suppress transcripts encoding proinflammatory cytokines within ILC2s.

## Materials and Methods

### Animal Care and Treatment

All mouse studies were performed with approval from the animal care and use committees of the National Institute of Environmental Health Sciences and West Virginia University. All mice used in these studies were maintained on a congenic C57BL/6J genetic background except *Il33* knock-out (KO) mice, which were maintained on a congenic C57BL/6N genetic background. C57BL/6J, *Rag1* KO, and *Thy1.1* (CD90.1) mice were purchased from Jackson Laboratories (stock numbers 000664, 002216, and 000406, respectively; Bar Harbor, MA). *Il33* KO (*Il33*<sup>tm1(KOMP)Vlcg</sup>) mice were obtained from the trans-National Institutes of Health Knock-Out Mouse Project Repository (University of California, Davis). Mice were administered standard chow and water *ad libitum* and maintained in a temperature- and humidity-controlled room with standard 12-hour light/dark cycles. For all experiments, sham, adrenalectomy, and castration surgeries were performed at 8 weeks of age. After adrenalectomy, mice were maintained on 0.85% saline drinking water to maintain ionic homeostasis. Also, 10 mg DHT 60-day sustained release pellets (Innovative Research of America, Sarasota, FL) or placebo pellets were implanted subcutaneously either during the adrenalectomy procedure (Figure 3) or 1-month post-adrenalectomy (Figure 4). To examine if steroid treatment suppresses proinflammatory cytokines within ILC2s, adrenalectomized + castrated (ADX + Cast) mice were aged 5 days after surgery to allow clearing of endogenous steroids and then administered a single intraperitoneal injection of dexamethasone or DHT (Steraloids, Newport, RI). The mice were humanely killed 3 hours after treatment. Control mice received vehicle (1x phosphate-buffered saline [PBS]). Both steroids were used at a 1 mg/kg concentration.

### Tissue Preparation

The gastric corpus lesser curvature was used for all analyses; a representative schematic is in [Supplementary Figure 1A](#). Stomachs were opened along the greater curvature and washed in PBS to remove the gastric contents. Stomachs used for histology were pinned to cork boards and fixed overnight in 4% paraformaldehyde at 4°C. After fixation, stomachs used for cryosectioning were cryopreserved in 30% sucrose and then embedded in optimal cutting temperature media. Stomachs used for paraffin sectioning were processed,

embedded, sectioned, and H&E stained according to standard protocols. For RNA isolation, the gastric corpus lesser curvature was collected with a 4-mm biopsy punch and immediately snap-frozen in liquid nitrogen. RNA was extracted in TRIzol (ThermoFisher, Waltham, MA) and precipitated from the aqueous phase using 1.5 volumes of 100% ethanol. The mixture was transferred to a RNeasy column (Qiagen, Hilden, Germany), and the remaining steps were followed according to the RNeasy kit manufacturer's recommendations. RNA was treated with RNase free DNase I (Qiagen) as part of the isolation procedure.

### Histology

Five-micrometer cryosections from the gastric corpus lesser curvature were incubated with ATP4B (clone 2G11, ThermoFisher), MIST1 (Cell Signaling Technologies, Danvers, MA), CD45 (clone 104 Biolegend, San Diego, CA), or CD44v9 (Cosmo Bio, Tokyo, Japan) for 1 hour at room temperature or overnight at 4°C. Primary antibody was omitted as a negative control. Sections were incubated in secondary antibodies for 1 hour at room temperature. Fluorescent conjugated *Griffonia simplicifolia* lectin (GSII; ThermoFisher) was added with secondary antibodies. Sections were mounted with Vectastain mounting media containing DAPI (Vector Laboratories, Burlingame, CA). Images were obtained using a Zeiss 880 confocal laser-scanning microscope (Carl-Zeiss GmbH, Jena, Germany) and running Zen Black imaging software. For AR immunohistochemistry, paraffin sections were probed with anti-AR antibodies (EPR1535(2), Abcam, Cambridge, United Kingdom) overnight at 4°C using the Vectastain ABC-HRP kit (Vector Laboratories). 3,3'-diaminobenzidine was used for detection (Vector Laboratories). Staining with isotype control antibodies were used as a negative control. Human stomach sections were obtained from the West Virginia University tissue bank. H&E- and immunohistochemistry (IHC)-stained paraffin sections were imaged using an Aperio AT2 Scanner (Leica Biosystems Inc., Buffalo Grove, IL). Parietal cells and chief cells were quantitated as previously described<sup>10</sup> using confocal micrographs captured using a 20x microscope objective and 1-μm-thick optical sections. Cells were counted using the ImageJ (National Institutes of Health, Bethesda, MD) count tool. Cells that stained positive with anti-ATP4B antibodies were identified as parietal cells, whereas cells that stained positive with anti-MIST1 antibodies and were GSII-negative were identified as mature chief cells. Counts were reported as the number of cells observed per 20x field. Images were chosen that contain gastric glands cut longitudinally. The first 5–6 glands adjacent to the limiting ridge were excluded from quantitation because they often exhibit an abnormal morphology.

### Flow Cytometry

To isolate leukocytes from the stomach, mice were humanely killed, and the stomachs were removed as described. The corpus was washed in Hank's Balanced Salt Solution without Ca<sup>2+</sup> or Mg<sup>2+</sup> containing 5 mmol/L HEPES, 5 mmol/L EDTA, and 5% fetal bovine serum at 37°C. Tissue was then washed in Hank's Balanced Salt Solution with Ca<sup>2+</sup> and Mg<sup>2+</sup> for 10 minutes at 37°C and then digested in 1 mg/mL type 1 collagenase and 0.5 mg/mL DNase I (Worthington Biochemical,



Lakewood, NJ) for 20 minutes at 37°C. After digestion, the tissue fragments were pushed through a 100- $\mu$ m strainer. Fc receptors were blocked with TruStain (BioLegend) and then stained with the antibodies listed in [Supplementary Table 1](#) for 20 minutes at 4°C. Actinomycin D (ThermoFisher) was used to label dead cells. Cells were analyzed on a BD Fortessa (BD Bioscience). For cells sorted from the small intestines, the small intestines were removed and flushed with PBS. The intestines were disassociated using the Lamina Propria Dissociation Kit (Miltenyi Biotec, Bergisch Gladbach, Germany) following the manufacturer's instructions. Intestinal cells were stained with the antibodies found in [Supplementary Table 1](#) as described and sorted on a FACS Aria III cell sorter (BD Bioscience) using the gating strategy in [Supplementary Figure 6](#). The data was analyzed using Cytobank software (Cytobank Inc., Santa Clara, CA). RNA was isolated using a NucleoSpin RNA kit (Takara Bio USA Inc., Mountain View, CA).

### T-Cell Transfer and ILC2 Depletion

Prior to ILC2 depletion, *Rag1* KO mice received an intravenous injection of 5 million splenic T cells isolated from *Thy1.1* mice through the lateral tail vein. ILC2s were depleted from *Rag1* KO mice using CD90.2 antibodies. The mice received 7 intraperitoneal injections containing 200  $\mu$ g of CD90.1 antibodies (Clone 30H12, BioXCell, Lebanon, NH) or isotype immunoglobulin G control antibodies (clone MPC-11) every 2 days for 14 days. Four days after T-cell transfer and the first antibody dose, the mice underwent sham surgery or ADX + Cast. The mice were humanely killed for analysis 10 days after surgery (schematic in [Figure 6A](#)).

### Single-cell RNAseq

Single-cell RNA sequencing (scRNAseq) was performed on pooled leukocytes isolated from the gastric corpus of 4 mice per treatment group. Viable CD45+ cells were sorted using a FACS Aria II (BD Bioscience, San Jose, CA) running FACS Diva software and resuspended at a concentration of  $1.0 \times 10^6$  cells/mL in RPMI 1640 + 10% fetal bovine serum. Single-cell libraries were prepared on a 10x Genomics Chromium controller (10x Genomics, Pleasanton, CA) using the version 3 reagent kit according to the manufacturer's instructions. The reagent mixture was calculated for capturing 6000 cells. The libraries were sequenced on a NovaSeq (Illumina, San Diego, CA) by the National Institute of Environmental Health Sciences Epigenomics core laboratory. Raw read processing was carried out using the Cell Ranger Single-Cell Software Suite (version 3.0.1, 10X Genomics). Demultiplexed FASTQ files (paired-end reads 1:30 base pairs [bp], read 2:100 bp) were generated using the CellRanger *mkfastq* command. The primary data analyses, which included alignment, filtering, barcode counting and unique molecular identifier (UMI) quantification, quality control, clustering and statistical analysis, were performed using CellRanger *count* command. Gene positions were annotated using Ensembl build 93 and filtered for biotype. Raw gene expression matrices were imported into R (version 3.6.1) and converted to a Seurat object using the Seurat R package (version 3.1.0).<sup>31</sup> To remove dead cells and doublets, the total number of UMIs and genes and the percentage of UMIs derived from the mitochondrial genome for each cell were counted. The

upper and lower bounds were defined as the mean  $\pm$  2 standard deviations for both the total UMIs and genes, respectively. Cells that had >10% UMIs derived from the mitochondrial genome were discarded. Finally, cells with total UMIs or genes outside of the upper and lower bounds were removed. For the remaining cells, gene expression matrices were normalized to the total cellular read count and to the mitochondrial read count. Highly variable genes were selected from the normalized data using the Seurat *SCTransform* function. The top 3000 highly variable genes were used as features for dimensionality reduction and clustering. The Seurat *RunPCA* and *JackStraw* functions were performed to calculate and to select significant ( $P < .05$ ) principal components, respectively. The *RunUMAP* function was then applied to plot the selected significant principal components. The *FindNeighbors* constructed a Shared Nearest Neighbor graph, and *FindClusters* function with "resolution = 0.1" parameter was carried out to cluster cells into different groups. Marker genes were defined based on the following criteria: (1) the average expression value in the cluster of interest was at least 1.2-fold higher than the average expression in the rest of the clusters; (2) >10% of cells in the cluster of interest, which were detectable; and (3) marker genes had the highest mean expression in the cluster of interest compared with the rest of the clusters. Canonical marker genes were used to annotate cell clusters.

### Quantitative Reverse Transcription-Polymerase Chain Reaction

Reverse transcription (RT) followed by quantitative polymerase chain reaction (qPCR) was performed in the same reaction using the Universal Probes One-Step PCR kit (Bio-Rad Laboratories) and the Taqman primers *Cftr* (Mm00445197\_m1), *Olfm4* (Mm01320260\_m1), *Wfdc2* (Mm00509434\_m1), *Il13* (Mm00434204\_m1), *Csf2* (Mm01290062\_m1), *Ar* (Mm00442688\_m1), and *Nr3c1* (Mm00433832\_m1) (ThermoFisher) on a CFX96 Real Time PCR system (Bio-Rad Laboratories). Messenger RNA (mRNA) levels were normalized to the reference gene *Ppip* (Mm00478295\_m1).

### Statistical Analysis

All error bars are  $\pm$  the standard deviation of the mean. The sample size for each experiment is indicated in the figure legends. Experiments were repeated a minimum of 2 times. Statistical analyses were performed using 1-way analysis of variance with post-hoc Tukey *t* test when comparing 3 or more groups or using unpaired *t* test when comparing 2 groups. Statistical analysis was performed using Graphpad Prism 9 software. Statistical significance was set at  $P \leq .05$ . Specific *P* values are listed in the figure legends.

## Results

### Glucocorticoids are Required to Suppress Gastric Inflammation in Females but are Dispensable in Males

We previously reported that glucocorticoids are master regulators of gastric inflammation and that global disrupt-



tion of glucocorticoid signaling triggers spontaneous gastric inflammation and SPEM.<sup>10</sup> To determine how sex impacts gastric inflammation, we adrenalectomized C57B6/J mice and aged them for 2 months after surgery. Female mice exhibited prominent mucosal thickening and chronic inflammation through the entire gastric corpus lesser curvature (Figure 1A and Supplementary Figure 1B). In contrast, the stomachs of adrenalectomized male mice were histologically normal. To determine if male resistance to ADX-induced gastric inflammation involved male sex hormones, male mice were either castrated alone or simultaneously ADX + Cast. The stomachs of castrated males did not exhibit gross histologic abnormalities (Figure 1A). However, ADX + Cast mice developed prominent histologic lesions that appeared identical to adrenalectomized female mice. Further analysis of discrete cell populations within the gastric glands demonstrated that 86% of parietal cells and 97% of chief cells were lost in adrenalectomized females, but these cell populations were not significantly reduced in adrenalectomized or castrated males (Figure 1B and 1C). In contrast, 80% of parietal cells and 99% of chief cells were lost in ADX + Cast males.

**Chronic gastric inflammation and oxyntic atrophy are linked to SPEM development.** SPEM development was confirmed using immunostaining for the SPEM marker CD44 variant 9 (CD44v9), demonstrating that SPEM only developed in adrenalectomized females and ADX + Cast males (Figure 2A). In addition, qRT-PCR of RNA isolated from the gastric corpus revealed that the characteristic SPEM markers *Cfr*, *Olfm4*, and *Wfdc2* were significantly induced in adrenalectomized females and ADX + Cast males (Figure 2B), but these genes were not significantly increased in either adrenalectomized or castrated males. Together, these results suggest that male sex hormones have an essential role in suppressing pathogenic gastric inflammation and metaplasia.

### Androgens Suppress Gastric Inflammation and Metaplasia

We next asked whether androgens can prevent ADX-induced gastric inflammation and metaplasia. Female mice were adrenalectomized and simultaneously implanted with a DHT sustained-release pellet or a placebo pellet (Figure 3A). Two months after surgery, adrenalectomized mice implanted with placebo pellets exhibited chronic inflammation, loss of parietal and chief cells, and chronic SPEM (Figure 3B and 3C and Supplementary Figure 2). DHT treatment completely blocked the development of gastric inflammation in adrenalectomized females. Moreover, DHT treatment prevented loss of parietal cells and chief cells and blocked SPEM development. Next, we asked if androgens could reverse ADX-induced gastric inflammation and SPEM. Female mice were aged 1 month after ADX or sham surgery to allow chronic inflammation and SPEM development. Mice were then implanted with a sustained-release DHT pellet and aged an additional month (Figure 4A). One month after surgery, ADX mice had oxyntic atrophy and SPEM

(Figure 4B and 4C). However, 1 month of DHT treatment completely reversed these pathologies. The stomachs of DHT-treated ADX mice were histologically indistinguishable from sham mice (Figure 4B) and exhibited the normal complement of parietal and chief cells (Figure 4C). These data demonstrate that androgens have potent anti-inflammatory effects within the stomach. Moreover, these data show that androgens can compensate for glucocorticoid insufficiency by controlling gastric inflammation.

### Androgens Signal Through ILC2s

Because DHT treatment suppressed gastric inflammation, we next sought to identify the cell populations within the stomach that respond to androgens. Immunoblot analysis of protein lysates from the gastric corpus exhibited equivalent expression of the AR within male and female stomachs (Figure 5A). We then performed IHC to identify AR-positive cell populations within the stomach. IHC revealed that the AR was not detectable within the gastric epithelial cells (Figure 5B). However, AR-positive cells were scattered between the gastric glands and within the lamina propria that were morphologically similar to leukocytes. A similar AR-expression pattern was observed in gastric biopsy specimens from human patients (Supplementary Figure 3). Based on these observations, we performed scRNAseq of CD45-positive cells isolated from the gastric corpus using flow cytometry. Leukocytes were isolated from male and female mice 2 months after sham surgery, ADX, and ADX + Cast. After sequencing, cells were dimensionally reduced into clusters using the unbiased Uniform Manifold Approximation and Projection algorithm, which identified 9 distinct cell clusters (Figure 5C). Each cell cluster was annotated based on the unique expression of characteristic marker genes, and representative genes were visualized as a dot plot (Figure 5D). Approximately 50% of stomach leukocytes in sham mice were macrophages (Figure 5E). However, the proportion of macrophages decreased in ADX and ADX + Cast mice due to expansion of the granulocyte, mast cell, and B-cell populations. Several recent studies, including our previous work, have demonstrated that macrophages are required to induce SPEM development. Surprisingly, our scRNAseq revealed that *Ar* mRNA was not detected within the macrophage cluster (Figure 5F). Rather, *Ar* expression was restricted to T cells, natural killer cells, ILC2s, and fibroblasts. In contrast, the GR transcript (*Nr3c1*) was ubiquitously expressed by all of the cell populations (Figure 5F). Interestingly, the relative expression of both the *Ar* and *Gr* was highest within the ILC2 cluster.

### ILC2s are Critical Regulators of Gastric Inflammation

Pathogenic macrophage activation drives SPEM development.<sup>10,22</sup> However, our scRNAseq data demonstrated that macrophages do not express detectable *Ar* mRNA. Recently, it was shown that ILC2s are required for SPEM development in L365 treated mice.<sup>11</sup> Because ILC2s express abundant *Ar* and *Gr*, we hypothesized that ILC2s

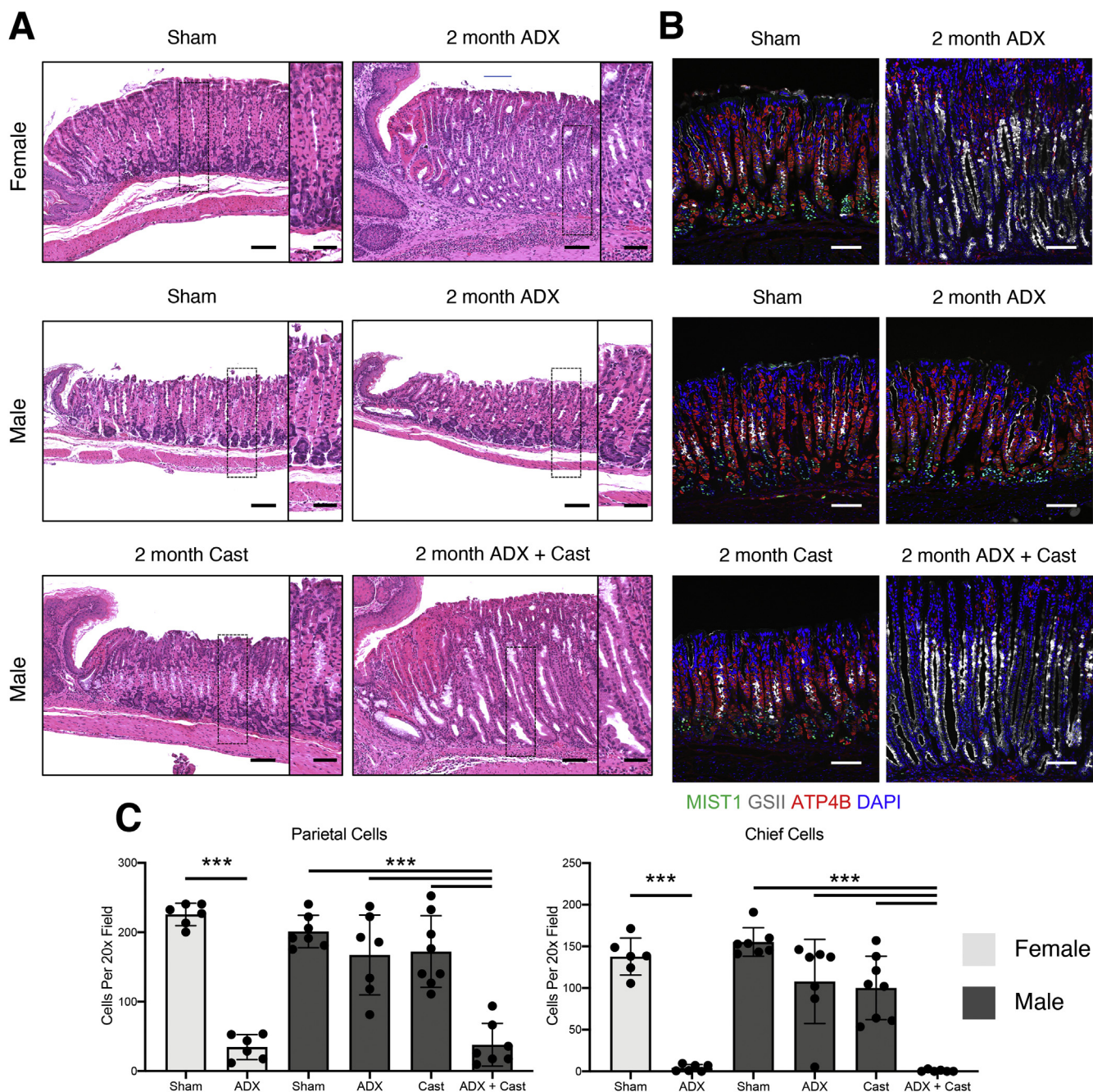


**Figure 1.** Glucocorticoids are dispensable in males for suppressing gastritis. Stomachs were collected from mice 2 months after surgery. (A) Representative micrographs of H&E-stained sections of the gastric corpus. Scale bars are 100  $\mu$ m and 50  $\mu$ m in the inset. (B) Immunostaining of stomach sections probed for ATP4B (parietal cells, red), GSII lectin (mucous neck cells, white), and MIST1 (chief cells, green). Nuclei are stained with DAPI. Scale bars are 100  $\mu$ m. (C) Quantitation of the number of parietal cells and chief cells observed per 20x field ( $n \geq 6$  mice/group). Data are mean  $\pm$  SD;  $P$ -values were determined using 1-way analysis of variance with post hoc Tukey  $t$  test. \*\*\* $P \leq .0001$ .

regulate gastric inflammation and SPEM development. To test this hypothesis, we depleted ILC2s by injecting CD90.2 antibodies (Figure 6A). CD90 is expressed by both ILC2s and T cells. Therefore, we used *Rag1* KO mice, which lack mature B and T cells. We previously showed that ADX-induced SPEM development occurs normally in *Rag1* KO mice.<sup>10</sup> However, because gastric T cells express *Ar*, we replace the gastric T-cell compartment by adoptive transfer of CD90.1 T cells that were spared by CD90.2

antibody treatment.<sup>32</sup> CD90.2 antibody treatment significantly reduced the gastric ILC2 population by 50% relative to mice treated with isotype control antibodies (Figure 6B), but the transferred CD90.1 T cells and macrophages, eosinophils, and natural killer cells were not affected by antibody injection (Figure 6B and Supplementary Figure 4). Ten days after surgery, ADX + Cast mice exhibited a significant 71% loss of parietal and a 91% loss of chief cells (Figure 6C and 6D) and



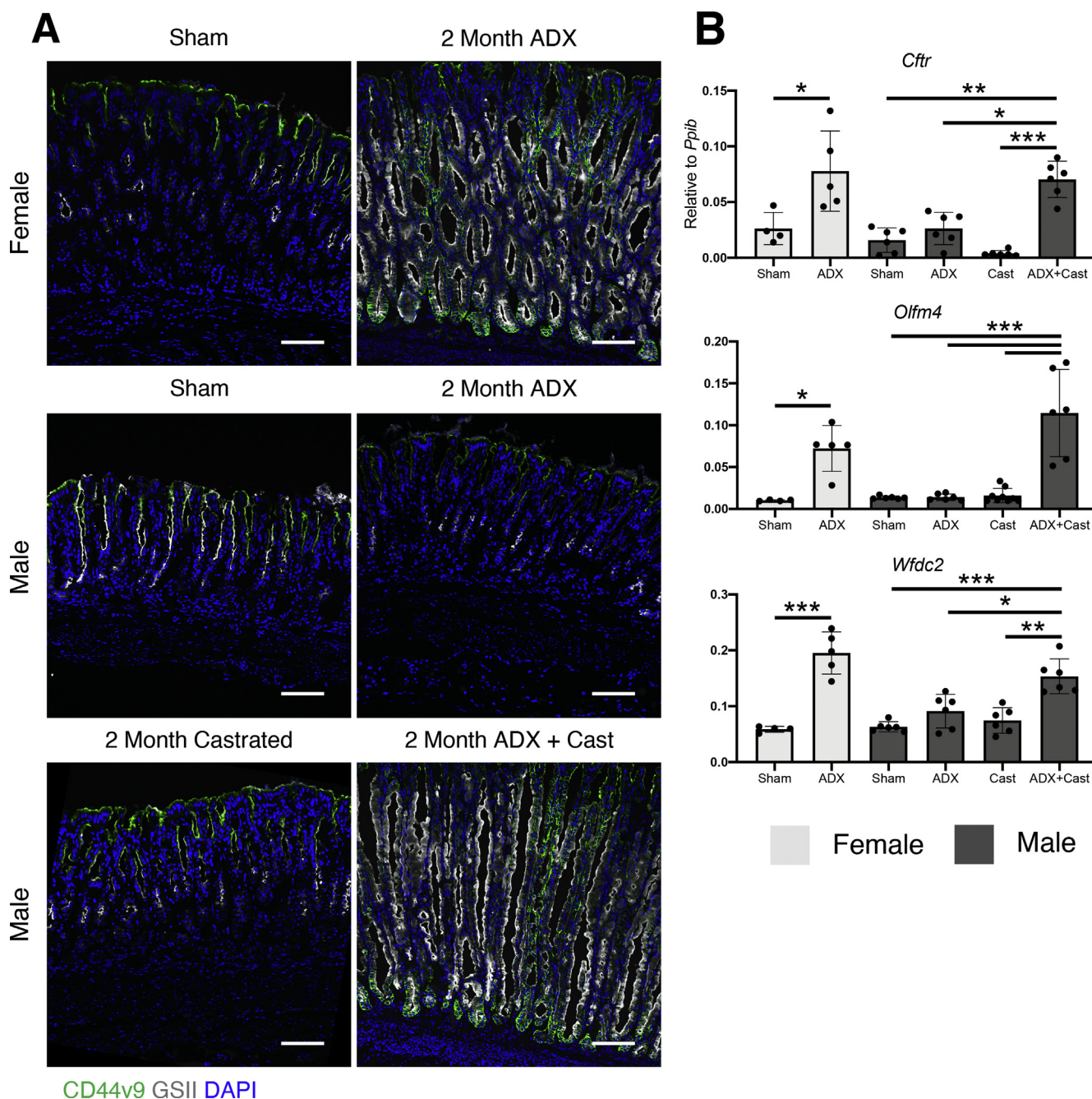


**Figure 2.** Glucocorticoids are required to suppress spontaneous SPEM in females but are dispensable in males. (A) Immunostaining for the SPEM marker CD44 variant 9 (green), mucous neck cells are stained with GSII lectin (white). Nuclei are stained with DAPI. Scale bars are 100  $\mu$ m. (B) Quantitative RT-PCR of the indicated SPEM marker genes using RNA isolated from the gastric corpus ( $n \geq 4$  mice/group). Data are mean  $\pm$  SD;  $P$ -values were determined using 1-way analysis of variance with post hoc Tukey  $t$  test. \* $P \leq .01$ ; \*\* $P \leq .001$ ; \*\*\* $P \leq .0001$ .

widespread induction of the SPEM marker CD44v9 (Figure 6C). In contrast, ILC2 depletion suppressed these ADX + Cast-induced pathologies preventing parietal and chief cell loss and CD44v9 induction.

To further test the role of ILC2s in gastric inflammation and SPEM development, we evaluated if impaired ILC2 function could protect from pathogenic inflammation-induced SPEM. To achieve this, we used *Il33* KO mice. IL33 is an alarmin that drives ILC2 proliferation and

activation.<sup>33</sup> In WT mice, IL33 is constitutively expressed by surface mucous (pit) cells within the gastric corpus (Supplementary Figure 5A). We found that during steady-state conditions, *Il33* KO males had significantly fewer tissue-resident ILC2s within the gastric corpus (Supplementary Figure 5B). Ten days after ADX + Cast, *Il33* KO mice were resistant to parietal and chief cell loss, whereas WT controls exhibited a significant 47% loss of parietal cells and an 87% loss of chief cells (Supplementary



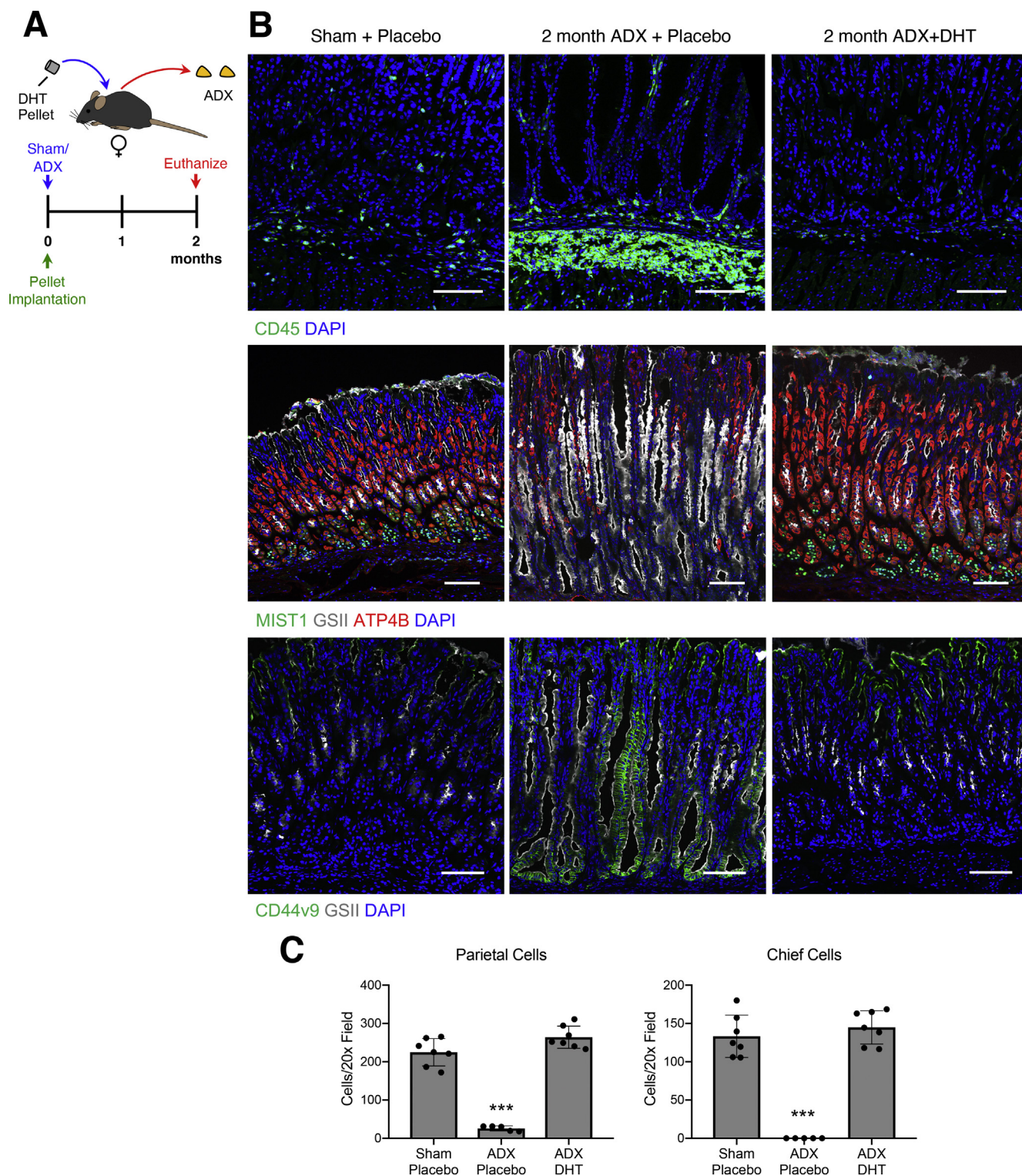


**Figure 3.** Androgens suppress gastric inflammation and SPEM after adrenalectomy. (A) Experimental model: female mice were adrenalectomized and simultaneously implanted with a sustained-release DHT pellet. Stomachs were collected 2 months after surgery. (B) Immunostaining of stomach sections probed for CD45 (pan-leukocytes, green), for ATP4B (parietal cells, red), GSII lectin (mucous neck cells, white), and MIST1 (chief cells, green), or for CD44v9 (SPEM, green) and GSII lectin (white). Nuclei are stained with DAPI. Scale bars are 100  $\mu$ m. (C) Quantitation of the number of parietal cells and chief cells observed per 20x field ( $n \geq 5$  mice/group). Data are mean  $\pm$  SD;  $P$ -values were determined using 1-way analysis of variance with post hoc Tukey  $t$  test. \*\*\* $P \leq .0001$ .

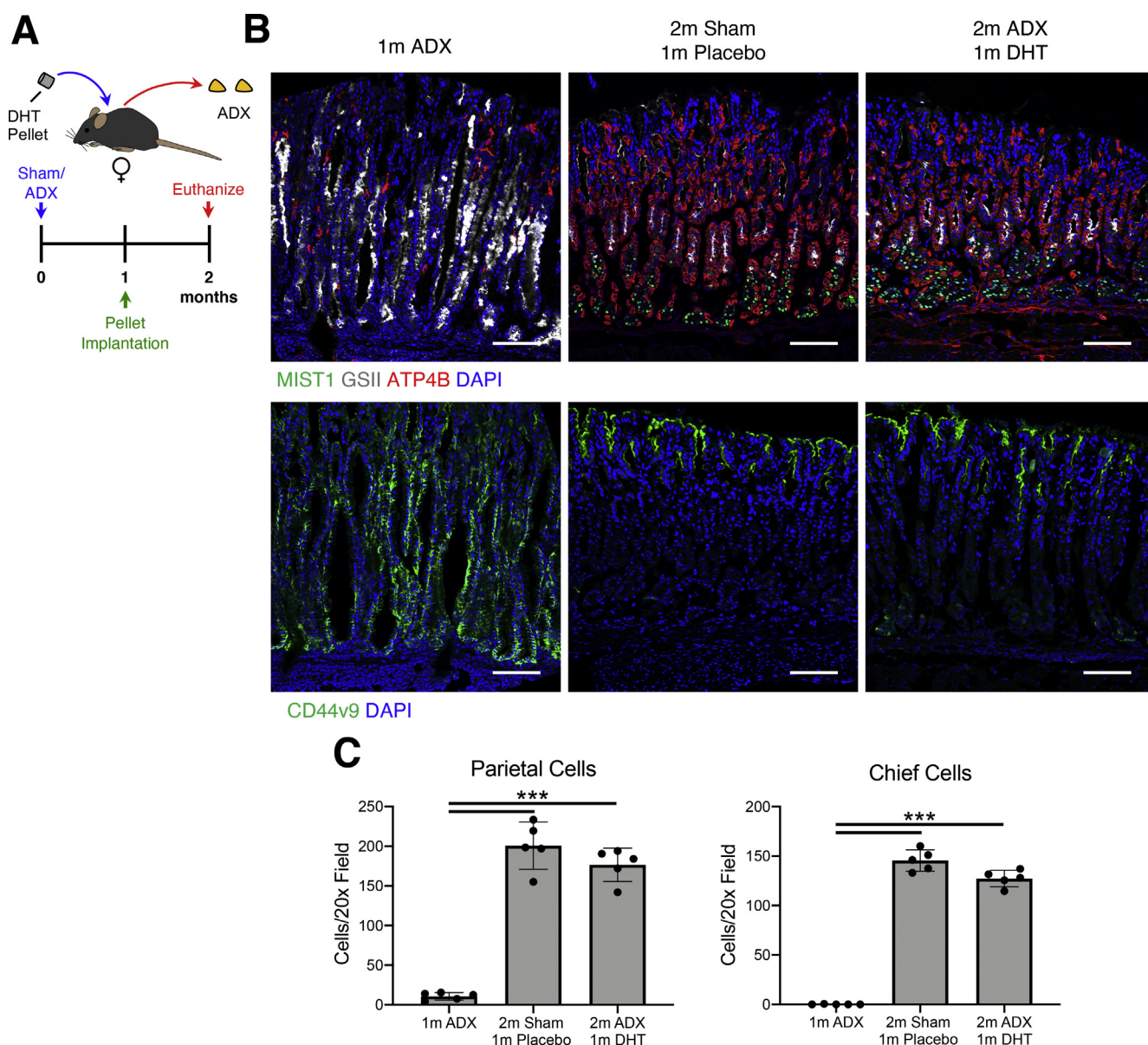


**Figure 4.** Androgen treatment reverses chronic SPEM in female mice. (A) Experimental design. Female mice were aged 1 month after sham surgery or adrenalectomy. They were then implanted with a sustained release DHT pellet or placebo controls and then were aged for an additional month. (B) Immunostaining of stomach sections probed for (B) ATP4B (parietal cells, red), GSII lectin (mucous neck cells, white), and MIST1 (chief cells, green) or for (C) CD44v9 (SPEM, green). Nuclei are stained with DAPI. Scale bars are 100  $\mu$ m (D) Quantitation of the number of parietal cells and chief cells observed per 20x field ( $n \geq 5$  mice/group). Data are mean  $\pm$  SD;  $P$ -values were determined using 1-way analysis of variance with post hoc Tukey  $t$  test. \*\*\* $P \leq .0001$ .

Figure 5C and 5D). Moreover, *Il33* KO mice had limited induction of the SPEM marker CD44v9 compared with widespread SPEM development in ADX + Cast WT controls (Supplementary Figure 5C). These data further demonstrate that ILC2s are important for initiating pathogenic gastric inflammation and SPEM.

### Androgens Signal Within ILC2s to Suppress Cytokine Production

Because ILC2s are required to induce SPEM, we next asked if androgens could suppress the expression of

transcripts encoding proinflammatory cytokines within ILC2s. Analysis of the scRNAseq data revealed that *Il13* and *Csf2* were abundant within ILC2s (Figure 7A). These transcripts are well-known direct targets of glucocorticoids<sup>34,35</sup> and the receptors for these cytokines are widely expressed by gastric leukocytes (Figure 7A). Moreover, IL13 has previously been shown to be required to induce SPEM development in L635 treated mice.<sup>16</sup> Therefore, we used the cytokines *Il13* and *Csf2* to assess the ability of androgens to suppress the expression of proinflammatory genes within ILC2s. Quantitative RT-PCR demonstrated a significant increase in *Il13* and *Csf2* mRNA within the gastric corpus of



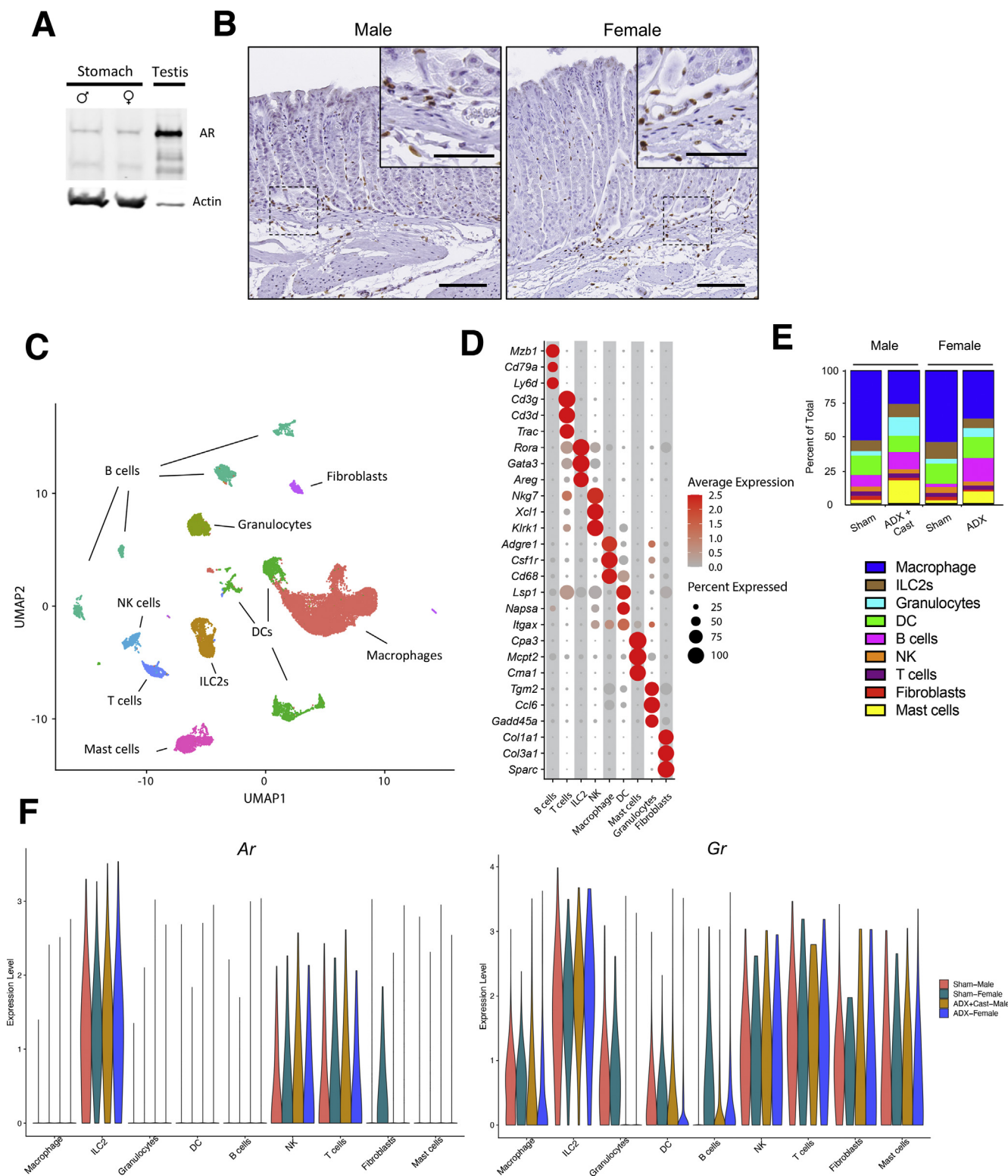


**Figure 5.** Gastric ILC2s express abundant AR and GR. (A) Immunoblot for the AR using protein isolated from the gastric corpus of male or female mice or the testis probed. (B) IHC of the gastric corpus stained with anti-AR antibodies. Scale bars are 100  $\mu$ m and 50  $\mu$ m in the inset. (C) UMAP unbiased clustering of scRNAseq performed using CD45<sup>+</sup> cells isolated from the gastric corpus from sham males, ADX + Cast males, sham females, and ADX females 2 months after surgery (n = 4). (D) Cell clusters annotated based on their expression of characteristic marker genes. Dot size represents the percentage of positive cells within a cluster and dot color represents the relative gene expression. (E) Ratios of each cell population in each treatment group. Total = 100%. (F) Violin plots of relative *Ar* and *Gr* expression within cell clusters stratified by treatment group.



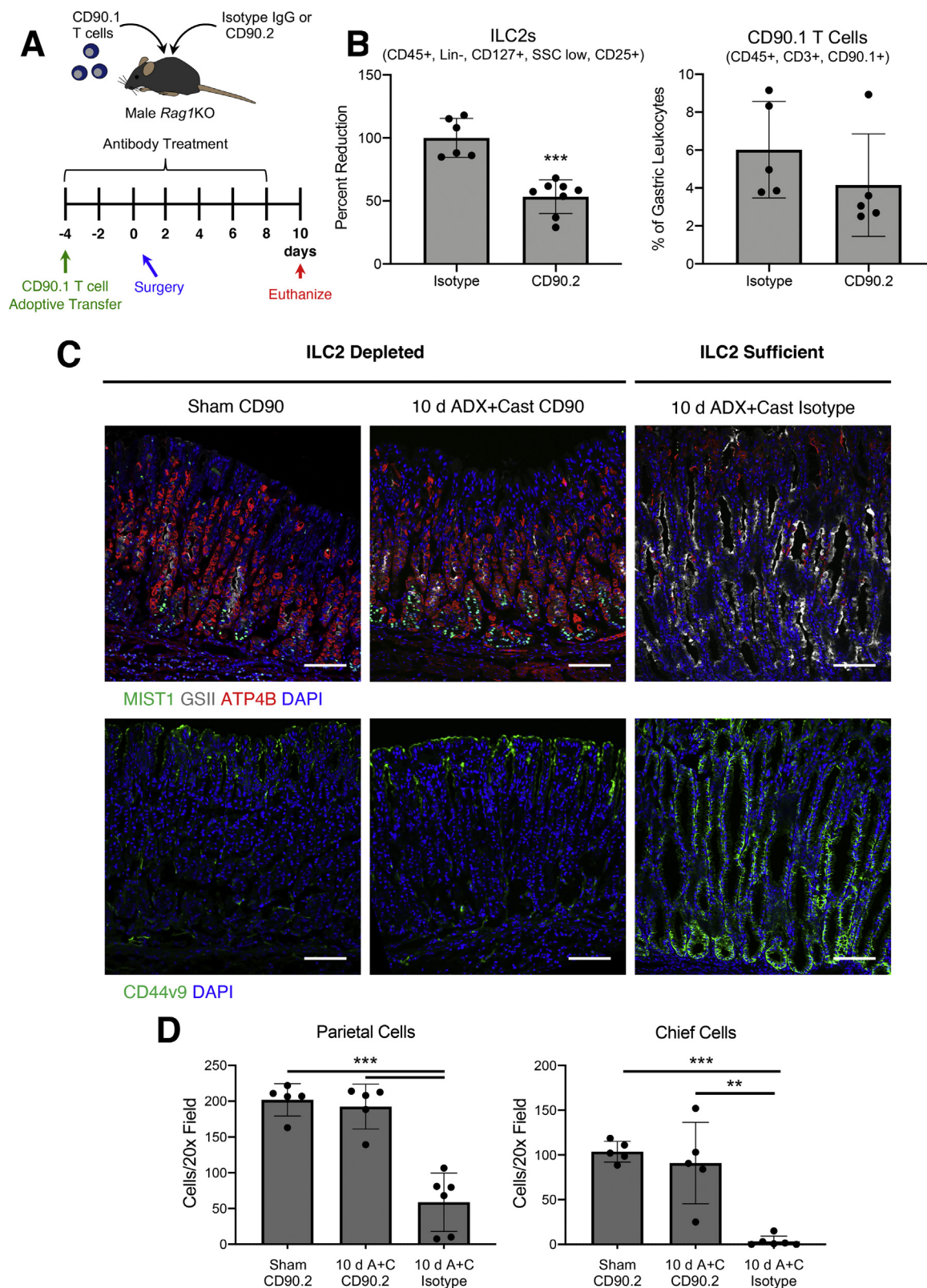
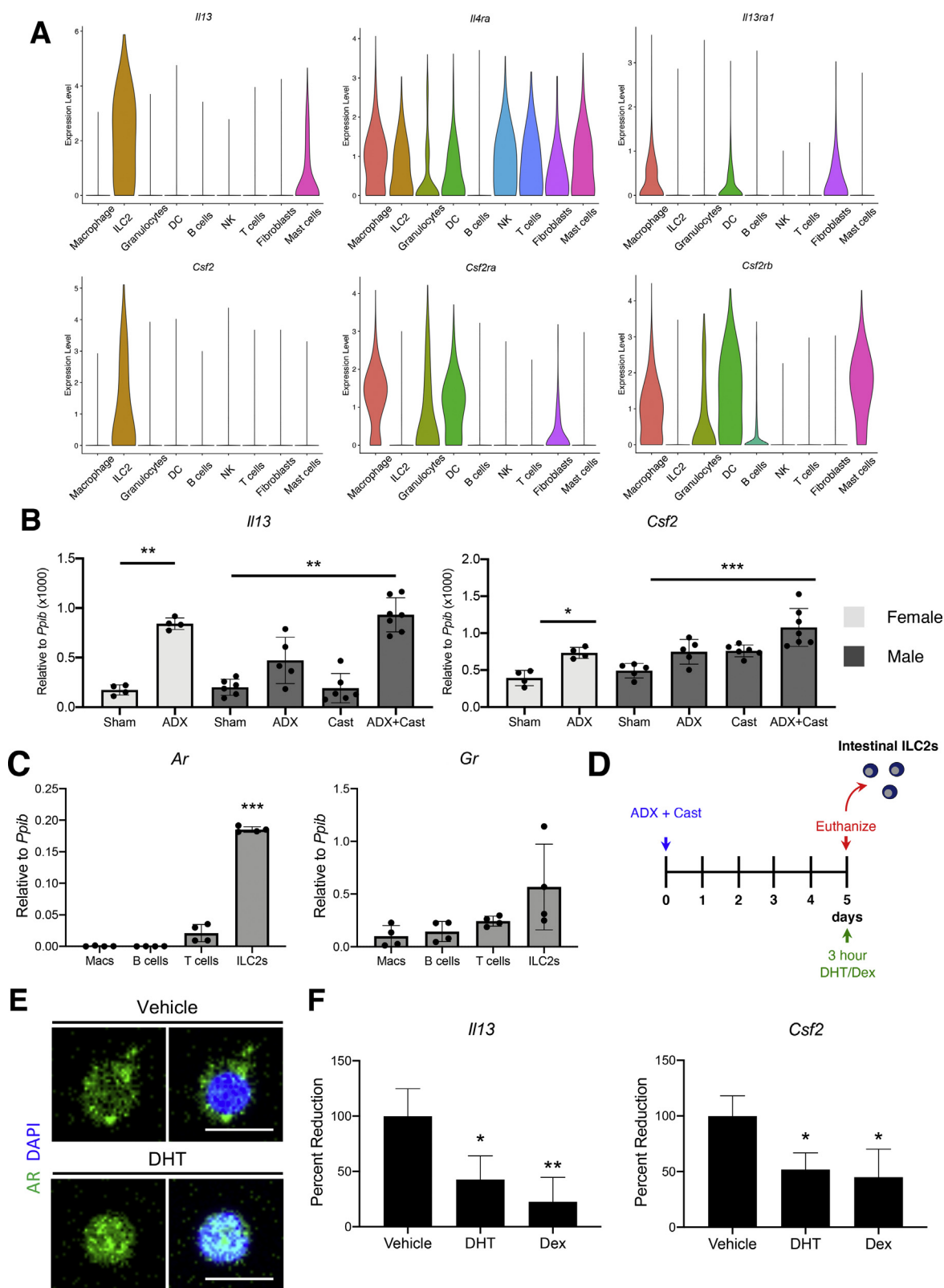


**Figure 6.** ILC2 depletion protects from SPEM development. (A) Experimental model: CD90.1 T cells were adoptively transferred into *Rag1* KO mice 4 days before surgery. In addition, mice were treated with CD90.2 or isotype control antibodies every 2 days throughout the experiment beginning 4 days before surgery. Stomachs were collected for analysis 10 days after sham surgery or adrenalectomy + castration. (B) Flow cytometry analysis of the gastric corpus from sham mice treated with CD90.2 or isotype control antibodies. (C) Immunostaining of stomach sections probed for (C) ATP4B (parietal cells, red), GSII lectin (mucous neck cells, white), and MIST1 (chief cells, green) or for (D) CD44v9 (SPEM, green). Nuclei are stained with DAPI. Scale bars are 100  $\mu$ m (D) Quantitation of the number of parietal cells and chief cells observed per 20x field ( $n \geq 5$  mice/group). Data are mean  $\pm$  SD; *P*-values were determined using unpaired *t* test (B) or using 1-way analysis of variance with post hoc Tukey *t* test (D). \*\*\**P*  $\leq$  .0001.

adrenalectomized females and ADX + Cast males, but not in adrenalectomized or castrated males (Figure 7B). Next, we asked if *Il13* and *Csf2* were regulated by androgens or glucocorticoids. We used intestinal ILC2s for this procedure

due to the relatively few ILC2s present within the stomach. RNA was isolated from macrophages, B cells, T cells, and ILC2s sorted from the small intestine (see Supplementary Figure 6 for gating strategy) and analyzed using qRT-PCR.



Similar to stomach leukocytes, *Ar* mRNA was undetectable in macrophages and B cells, expressed at relatively low levels in T cells, but was abundant within ILC2s (Figure 7C). In contrast, *Gr* expression was equivalent in all of the cell populations. Next, ADX + Cast males were treated with a single intraperitoneal injection of either DHT or dexamethasone (Figure 7D). Three hours after injection, the mice were humanely killed, and ILC2s were collected from the small intestines. Immunostaining for the AR in isolated intestinal ILC2s demonstrated that AR was predominantly within the cytoplasm of vehicle-treated mice but markedly translocated to the nucleus upon treatment with DHT (Figure 7E), demonstrating the normal nuclear translocation of activated steroid hormone receptors. Quantitative RT-PCR of RNA isolated from intestinal ILC2s revealed that treatment with either DHT or dexamethasone significantly suppressed expression of both *Ilf3* and *Csf2* after 3 hours (Figure 7F). These results demonstrate a novel role for androgens in suppressing the expression of mRNAs encoding proinflammatory cytokines within ILC2s.

## Discussion

Biological sex has profound effects on inflammation, and a host of inflammatory syndromes and diseases are stratified by sex.<sup>5</sup> Females typically elicit a more robust inflammatory response to pathogens and have increased protection from infection.<sup>1</sup> Moreover, females develop higher antibody titers in response to vaccines.<sup>3</sup> In contrast, males have generally weaker inflammatory reactions and are more likely than women to die of infection.<sup>36</sup> The robust inflammatory response in females may come with an increased risk of inflammatory diseases, and 8 of 10 individuals with autoimmune disease are women.<sup>1</sup> Although many of these inflammatory diseases are multi-factorial, sex hormones play important roles in regulating inflammation. Before puberty, boys and girls exhibit similar asthma rates, but after puberty, the ratio of asthma in males becomes significantly lower, suggesting that increased androgens may be protective.<sup>37</sup> A similar trend is observed within the gastrointestinal tract where pre-puberal boys and girls have similar rates of Crohn's disease, but women exhibit higher rates than men.<sup>38,39</sup> Within the stomach, nonautoimmune, autoimmune, and eosinophilic gastritis are more common in women, but the etiology underlying these sex-specific effects in inflammatory disease are not clear.<sup>40</sup> Studies have found that bacterial infections by *H pylori* are more common

in men and that men have higher bacterial loads than women.<sup>7-9</sup> Although glucocorticoids are the primary anti-inflammatory steroid hormone, these hormones signal differently in males and females, in part due to interactions with sex steroid receptors.<sup>2,41,42</sup> Moreover, recent studies have found that androgens also have overt anti-inflammatory effects.<sup>24,25</sup> Indeed, within the lungs, androgens signal in ILC2s to suppress their activation and production of proinflammatory cytokines. However, the exact mechanisms by which sex influences the inflammatory response are poorly understood. Here, we report a novel role for androgens in regulating gastric inflammation. We found that adrenalectomized females develop pathogenic inflammation and SPEM. In contrast, the stomachs of adrenalectomized males remain normal due to the anti-inflammatory effects of androgens, which signaled within ILC2s to suppress the expression of genes encoding proinflammatory cytokines.

Glucocorticoids and androgens predominately signal through binding to the GR and AR, respectively. These receptors are ligand-dependent transcription factors that regulate gene transcription by binding DNA response elements to recruit initiation factors, chromatin modifiers, and RNA polymerase II.<sup>43</sup> The GR and AR are structurally similar to each other, and the DNA response elements bound by these receptors are nearly identical.<sup>26</sup> The GR and AR can readily bind each other's response elements in vitro, and GR and AR co-expression in immortalized cell lines demonstrates significant overlap in their target genes.<sup>44,45</sup> Moreover, expression of the GR in prostate cancer is thought to enable cancer cells to escape antiandrogen therapies by regulating the expression of AR target genes.<sup>30</sup> We demonstrate that the GR is ubiquitously expressed by all leukocytes, consistent with its established role in regulating inflammation. However, AR expression is much more restricted, suggesting a more nuanced role in regulating inflammation. ILC2s coexpress high levels of the GR and AR. Within ILC2s, treatment with either steroid suppressed expression of the proinflammatory cytokines *Ilf3* and *Csf2*. These mRNAs were significantly suppressed within 3 hours of DHT treatment. The short timeframe for this repression suggests that androgens are directly inhibiting these transcripts. The redundant functions of glucocorticoids and androgens may provide males with an extra layer of protection from inflammatory diseases and partially explain why men have lower rates of inflammatory and autoimmune diseases than women.

**Figure 7.** Androgens and glucocorticoids suppress proinflammatory cytokine production by ILC2s. (A) Violin plots of the indicated genes derived from the overlaid scRNAseq data of sham males, ADX + Cast males, sham females, and ADX females 2 months after surgery. (B) Quantitative RT-PCR of the indicated genes using RNA isolated from the gastric corpus ( $n \geq 4$  mice/group). (C) Quantitative RT-PCR of the *Ar* and *Gr* using RNA isolated from intestinal macrophages, B cells, T cells, and ILC2s ( $n = 8$ ). (D) Experimental model: male mice were adrenalectomized + castrated to clear endogenous hormones. Five days after surgery, mice received a single intraperitoneal injection of DHT or dexamethasone (Dex). Three hours after injection, the intestines were removed for isolation of discrete leukocyte populations. (E) Immunostaining of intestinal ILC2s isolated from ADX + Cast mice 3 hours after treatment with vehicle or DHT. Cells were stained with AR antibodies, and nuclei were stained with DAPI. Scale bar 10  $\mu$ m. (F) Quantitative RT-PCR of *Ilf3* and *Csf2* using RNA isolated from intestinal ILC2s. Experiments were repeated 3 times with cells pooled from  $\geq 2$  mice/group. All data are mean  $\pm$  SD; *P*-values were determined using 1-way analysis of variance with post hoc Tukey *t* test. \**P*  $\leq .05$ ; \*\**P*  $\leq .001$ ; and \*\*\**P*  $\leq .0001$ .



Several recent studies report that macrophages induce gastric damage and drive SPEM development.<sup>10,16,22</sup> Other studies suggest that androgens suppress macrophage activation.<sup>46</sup> However, we could not detect *Ar* mRNA within stomach macrophages using scRNAseq, or within intestinal macrophages using qRT-PCR. Although androgens may signal in macrophages through AR-independent mechanisms such as interacting with g-protein-coupled receptors, androgens also may impact macrophage activity indirectly by signaling in other cell populations. ILC2s are well known for their ability to induce and coordinate inflammation. Here, we demonstrate that gastric ILC2s express *Il13* and *Csf2*, cytokines that are known to modulate macrophage activity.<sup>47,48</sup> Recently, it was reported that IL13 activates gastric macrophages and is required to induce SPEM development.<sup>16</sup> Th2 T cells can also produce IL13, but ILC2s produce approximately 10-fold more IL13 than CD4+ Th2 T cells.<sup>20</sup> We previously showed that T-cell-deficient *Rag1* KO mice develop SPEM normally,<sup>10,22</sup> and we showed here that ILC2 depletion protects from SPEM development. Thus, ILC2s are ideally positioned within the stomach to regulate inflammation and macrophage activation, and androgen signaling within ILC2s likely shapes the gastric macrophage response.

Our data indicate that males are more resistant than females to gastric inflammation. *H. pylori*-induced chronic inflammation is thought to be the primary driver of gastric cancer development.<sup>12</sup> Metaplasia is also considered a potential precursor of gastric adenocarcinoma, although SPEM develops in response to a variety of glandular insults and may not progress to cancer. Here, we found that females were more susceptible to gastric inflammation and SPEM than males, but men are nearly 2 times more likely than women to develop gastric cancer.<sup>49</sup> Interestingly, the male bias in *H. pylori*-induced carcinogenesis is not always born out in animal studies. Some studies have found that male mice are more susceptible to *H. pylori*-induced gastric inflammation, mutation, and cancer<sup>50,51</sup>; others have found no male bias.<sup>8,52</sup> The increased rate of gastric cancer in men is partially attributed to lifestyle differences, with men consuming more alcohol and being more likely to smoke than women.<sup>53–55</sup> Age is another significant risk factor for gastric cancer.<sup>56</sup> Decreased androgen production during male menopause may increase cancer susceptibility later in life. Another possibility is that AR expression may change within the stomach during cancer development. We show that the gastric epithelium does not express detectable levels of the AR in samples from healthy mice and humans. However, a recent study found that 43% of gastric cancers were AR-positive.<sup>57</sup> AR-positive gastric cancers are associated with increased metastasis and decreased patient survival.<sup>58</sup> These features are reminiscent of prostate cancer, where androgens have different roles in healthy tissue and cancer. Thus, androgens may exert dual functions to protect from inflammatory and autoimmune diseases during normal conditions, but they may promote cancer growth and progression when dysregulated. Future studies will assess the role of glucocorticoids and sex hormones in regulating inflammation and cancer development during *H. pylori* infection.

## Supplementary Material

Note: To access the supplementary material accompanying this article, visit the online version of *Gastroenterology* at [www.gastrojournal.org](http://www.gastrojournal.org), and at <http://doi.org/10.1053/j.gastro.2021.04.075>.

## References

1. Fish EN. The X-files in immunity: sex-based differences predispose immune responses. *Nat Rev Immunol* 2008; 8:737–744.
2. Quinn M, Ramamoorthy S, Cidlowski JA. Sexually dimorphic actions of glucocorticoids: beyond chromosomes and sex hormones. *Ann N Y Acad Sci* 2014; 1317:1–6.
3. Fischinger S, Boudreau CM, Butler AL, et al. Sex differences in vaccine-induced humoral immunity. *Semin Immunopathol* 2019;41:239–249.
4. Klein SL, Flanagan KL. Sex differences in immune responses. *Nat Rev Immunol* 2016;16:626–638.
5. Ngo ST, Steyn FJ, McCombe PA. Gender differences in autoimmune disease. *Front Neuroendocrinol* 2014; 35:347–369.
6. El-Zimaity H, Riddell RH. Beyond *Helicobacter*: dealing with other variants of gastritis—an algorithmic approach. *Histopathology* 2021;78:48–69.
7. de Martel C, Parsonnet J. *Helicobacter pylori* infection and gender: a meta-analysis of population-based prevalence surveys. *Dig Dis Sci* 2006;51:2292–2301.
8. Sheh A, Lee CW, Masumura K, et al. Mutagenic potency of *Helicobacter pylori* in the gastric mucosa of mice is determined by sex and duration of infection. *Proc Natl Acad Sci U S A* 2010;107:15217–15222.
9. Ibrahim A, Morais S, Ferro A, et al. Sex-differences in the prevalence of *Helicobacter pylori* infection in pediatric and adult populations: systematic review and meta-analysis of 244 studies. *Dig Liver Dis* 2017;49:742–749.
10. Busada JT, Ramamoorthy S, Cain DW, et al. Endogenous glucocorticoids prevent gastric metaplasia by suppressing spontaneous inflammation. *J Clin Invest* 2019;129:1345–1358.
11. Meyer AR, Engevik AC, Madorsky T, et al. Group 2 innate lymphoid cells coordinate damage response in the stomach. *Gastroenterology* 2020;159:2077–2091.e8.
12. Meyer AR, Goldenring JR. Injury, repair, inflammation and metaplasia in the stomach. *J Physiol* 2018; 596:3861–3867.
13. Teal E, Dua-Awereh M, Hirshorn ST, et al. Role of metaplasia during gastric regeneration. *Am J Physiol Cell Physiol* 2020;319:C947–C954.
14. Miao ZF, Sun JX, Adkins-Threats M, et al. DDIT4 licenses only healthy cells to proliferate during injury-induced metaplasia. *Gastroenterology* 2021;160:260–271.e10.
15. Sáenz JB, Mills JC. Acid and the basis for cellular plasticity and reprogramming in gastric repair and cancer. *Nat Rev Gastroenterol Hepatol* 2018;15:257–273.
16. Petersen CP, Meyer AR, De Salvo C, et al. A signalling cascade of IL-33 to IL-13 regulates metaplasia in the mouse stomach. *Gut* 2018;67:805–817.

17. Germain RN, Huang Y. ILC2s - resident lymphocytes pre-adapted to a specific tissue or migratory effectors that adapt to where they move? *Curr Opin Immunol* 2019;56:76–81.
18. Hoyler T, Klose CS, Souabni A, et al. The transcription factor GATA-3 controls cell fate and maintenance of type 2 innate lymphoid cells. *Immunity* 2012;37:634–648.
19. Gour N, Smole U, Yong HM, et al. C3a is required for ILC2 function in allergic airway inflammation. *Mucosal Immunol* 2018;11:1653–1662.
20. Halim TY, Steer CA, Matha L, et al. Group 2 innate lymphoid cells are critical for the initiation of adaptive T helper 2 cell-mediated allergic lung inflammation. *Immunity* 2014;40:425–435.
21. Mindt BC, Fritz JH, Duerr CU. Group 2 innate lymphoid cells in pulmonary immunity and tissue homeostasis. *Front Immunol* 2018;9:840.
22. Petersen CP, Weis VG, Nam KT, et al. Macrophages promote progression of spasmodic polypeptide-expressing metaplasia after acute loss of parietal cells. *Gastroenterology* 2014;146:1727–1738.e8.
23. Becerra-Díaz M, Strickland AB, Keselman A, et al. Androgen and androgen receptor as enhancers of M2 macrophage polarization in allergic lung inflammation. *J Immunol* 2018;201:2923–2933.
24. Laffont S, Blanquart E, Savignac M, et al. Androgen signaling negatively controls group 2 innate lymphoid cells. *J Exp Med* 2017;214:1581–1592.
25. Cephus JY, Stier MT, Fuseini H, et al. Testosterone attenuates group 2 innate lymphoid cell-mediated airway inflammation. *Cell Rep* 2017;21:2487–2499.
26. Claessens F, Joniau S, Helsen C. Comparing the rules of engagement of androgen and glucocorticoid receptors. *Cell Mol Life Sci* 2017;74:2217–2228.
27. Cain DW, Cidlowski JA. Immune regulation by glucocorticoids. *Nat Rev Immunol* 2017;17:233–247.
28. Shaffer PL, Jivan A, Dollins DE, et al. Structural basis of androgen receptor binding to selective androgen response elements. *Proc Natl Acad Sci U S A* 2004;101:4758–4763.
29. van Tilborg MA, Bonvin AM, Hard K, et al. Structure refinement of the glucocorticoid receptor-DNA binding domain from NMR data by relaxation matrix calculations. *J Mol Biol* 1995;247:689–700.
30. Arora VK, Schenkein E, Murali R, et al. Glucocorticoid receptor confers resistance to antiandrogens by bypassing androgen receptor blockade. *Cell* 2013;155:1309–1322.
31. Butler A, Hoffman P, Smibert P, et al. Integrating single-cell transcriptomic data across different conditions, technologies, and species. *Nat Biotechnol* 2018;36:411–420.
32. Rafei-Shamsabadi DA, van de Poel S, Dorn B, et al. Lack of type 2 innate lymphoid cells promotes a type I-driven enhanced immune response in contact hypersensitivity. *J Invest Dermatol* 2018;138:1962–1972.
33. McHedlidze T, Waldner M, Zopf S, et al. Interleukin-33-dependent innate lymphoid cells mediate hepatic fibrosis. *Immunity* 2013;39:357–371.
34. Newton R, King EM, Gong W, et al. Glucocorticoids inhibit IL-1 $\beta$ -induced GM-CSF expression at multiple levels: roles for the ERK pathway and repression by MKP-1. *Biochem J* 2010;427:113–124.
35. Paranjape A, Chernushevich O, Qayum AA, et al. Dexamethasone rapidly suppresses IL-33-stimulated mast cell function by blocking transcription factor activity. *J Leukoc Biol* 2016;100:1395–1404.
36. Owens IP. Ecology and evolution. Sex differences in mortality rate. *Science* 2002;297:2008–2009.
37. Fröhlich M, Pinart M, Keller T, et al. Is there a sex-shift in prevalence of allergic rhinitis and comorbid asthma from childhood to adulthood? A meta-analysis. *Clin Transl Allergy* 2017;7:44.
38. Greuter T, Manser C, Pittet V, et al. Gender differences in inflammatory bowel disease. *Digestion* 2020;101(Suppl 1): 98–104.
39. Severs M, Spekhorst LM, Mangen MJ, et al. Sex-related differences in patients with inflammatory bowel disease: results of 2 prospective cohort studies. *Inflamm Bowel Dis* 2018;24:1298–1306.
40. Cabrera de León A, Almeida González D, Almeida AA, et al. Factors associated with parietal cell autoantibodies in the general population. *Immunol Lett* 2012;147: 63–66.
41. Quinn MA, Cidlowski JA. Endogenous hepatic glucocorticoid receptor signaling coordinates sex-biased inflammatory gene expression. *FASEB j* 2016;30:971–982.
42. Quinn MA, Xu X, Ronfani M, et al. Estrogen deficiency promotes hepatic steatosis via a glucocorticoid receptor-dependent mechanism in mice. *Cell Rep* 2018; 22:2690–2701.
43. Oakley RH, Cidlowski JA. The biology of the glucocorticoid receptor: new signaling mechanisms in health and disease. *J Allergy Clin Immunol* 2013;132:1033–1044.
44. De Vos P, Claessens F, Peeters B, et al. Interaction of androgen and glucocorticoid receptor DNA-binding domains with their response elements. *Mol Cell Endocrinol* 1993;90:R11–R116.
45. Sahu B, Laakso M, Pihlajamaa P, et al. FoxA1 specifies unique androgen and glucocorticoid receptor binding events in prostate cancer cells. *Cancer Res* 2013; 73:1570–1580.
46. Fuseini H, Newcomb DC. Mechanisms driving gender differences in asthma. *Curr Allergy Asthma Rep* 2017;17:19.
47. Hamilton JA. GM-CSF-dependent inflammatory pathways. *Front Immunol* 2019;10:2055.
48. Shapouri-Moghaddam A, Mohammadian S, Vazini H, et al. Macrophage plasticity, polarization, and function in health and disease. *J Cell Physiol* 2018;233:6425–6440.
49. Torre LA, Bray F, Siegel RL, et al. Global cancer statistics. 2012. *CA Cancer J Clin* 2015;65:87–108.
50. Fox JG, Rogers AB, Ihrig M, et al. Helicobacter pylori-associated gastric cancer in INS-GAS mice is gender specific. *Cancer Res* 2003;63:942–950.
51. Ohtani M, Garcia A, Rogers AB, et al. Protective role of 17  $\beta$ -estradiol against the development of Helicobacter pylori-induced gastric cancer in INS-GAS mice. *Carcinogenesis* 2007;28:2597–2604.
52. Sutton P, Wilson J, Genta R, et al. A genetic basis for atrophy: dominant non-responsiveness and helicobacter

- induced gastritis in F(1) hybrid mice. *Gut* 1999;45:335–340.
53. Yamaji Y, Watabe H, Yoshida H, et al. High-risk population for gastric cancer development based on serum pepsinogen status and lifestyle factors. *Helicobacter* 2009;14:81–86.
  54. Parascandola M, Xiao L. Tobacco and the lung cancer epidemic in China. *Transl Lung Cancer Res* 2019;8:S21–S30.
  55. Teixeira-Compano E, Espelt A, Sordo L, et al. Differences between men and women in substance use: the role of educational level and employment status. *Gac Sanit* 2018;32:41–47.
  56. Bray F, Ferlay J, Soerjomataram I, et al. Global cancer statistics 2018: GLOBOCAN estimates of incidence and mortality worldwide for 36 cancers in 185 countries. *CA Cancer J Clin* 2018;68:394–424.
  57. **Tang W, Liu R, Yan Y**, et al. Expression of estrogen receptors and androgen receptor and their clinical significance in gastric cancer. *Oncotarget* 2017;8:40765–40777.
  58. Kominea A, Konstantinopoulos PA, Kapranos N, et al. Androgen receptor (AR) expression is an independent unfavorable prognostic factor in gastric cancer. *J Cancer Res Clin Oncol* 2004;130:253–258.

---

Author names in bold designate shared co-first authorship.

Received March 21, 2020. Accepted April 27, 2021.

#### Reprint requests

Address requests for reprints to: Jonathan T. Busada, PhD, West Virginia University School of Medicine, Microbiology, Immunology and Cell Biology, 64 Medical Center Drive, PO Box 9177, Morgantown, West Virginia 26506. e-mail: [jonathan.busada@hsc.wvu.edu](mailto:jonathan.busada@hsc.wvu.edu); or John A. Cidlowski, PhD, Building

101 MD F3-07, 111 TW Alexander Drive, Research Triangle Park, North Carolina 27709. e-mail: [cidlows1@niehs.nih.gov](mailto:cidlows1@niehs.nih.gov).

#### Acknowledgments

The authors thank the National Institute of Environmental Health Sciences Comparative Medicine Branch, Histology Core Laboratory, Epigenomes Core Laboratory, Flow Cytometry Center, Fluorescence Microscopy Imaging Center, and NIEHS Arts and Graphics for their assistance. The authors also thank Sarah McLaughlin for technical assistance.

#### CRedit Authorship Contributions

Jonathan T. Busada, PhD (Conceptualization: Lead; Data curation: Lead; Formal analysis: Lead; Funding acquisition: Supporting; Investigation: Lead; Methodology: Lead; Project administration: Lead; Supervision: Lead; Validation: Lead; Visualization: Lead; Writing – original draft: Lead; Writing – review & editing: Lead)

Kylie N. Peterson, BS (Data curation: Supporting; Formal analysis: Supporting; Writing – review & editing: Supporting)

Stuti Khadka, MS (Data curation: Supporting; Formal analysis: Supporting; Writing – review & editing: Supporting)

Xiaojiang Xu, PhD (Formal analysis: Supporting; Resources: Equal; Software: Supporting; Visualization: Supporting; Writing – review & editing: Supporting)

Robert H. Oakley, PhD (Data curation: Supporting; Formal analysis: Supporting; Investigation: Supporting; Writing – review & editing: Supporting), Donald N. Cook, PhD (Methodology: Supporting; Resources: Supporting; Writing – review & editing: Supporting)

John A. Cidlowski, PhD (Conceptualization: Equal; Funding acquisition: Lead; Methodology: Supporting; Project administration: Supporting; Supervision: Supporting; Writing – review & editing: Supporting)

#### Conflicts of interest

The authors disclose no conflicts.

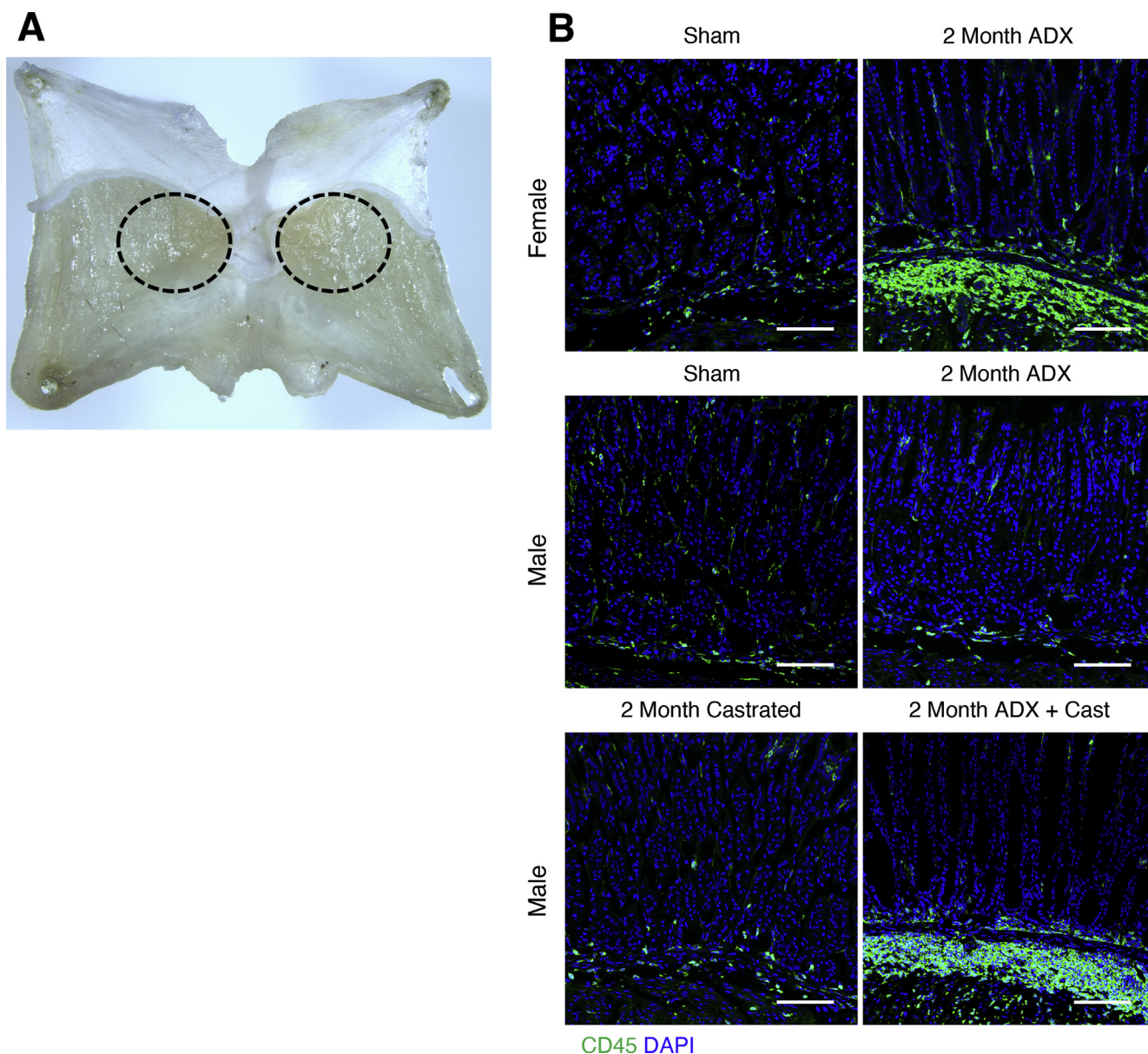
#### Funding

This research was supported by a Postdoctoral Research Associate fellowship from the National Institute of General Medical Sciences 1Fi2GM123974 (J.T.B.), by West Virginia University start-up funds (J.T.B.), and by the Intramural Research Program of the National Institutes of Health/NIEHS 1ZIAES090057 (J.A.C.). The West Virginia University Microscopy Imaging Facility and Flow Cytometry Core Facility are supported by National Institutes of Health grants P30GM103488, P20GM103434, U54GM104942, and P20GM121322

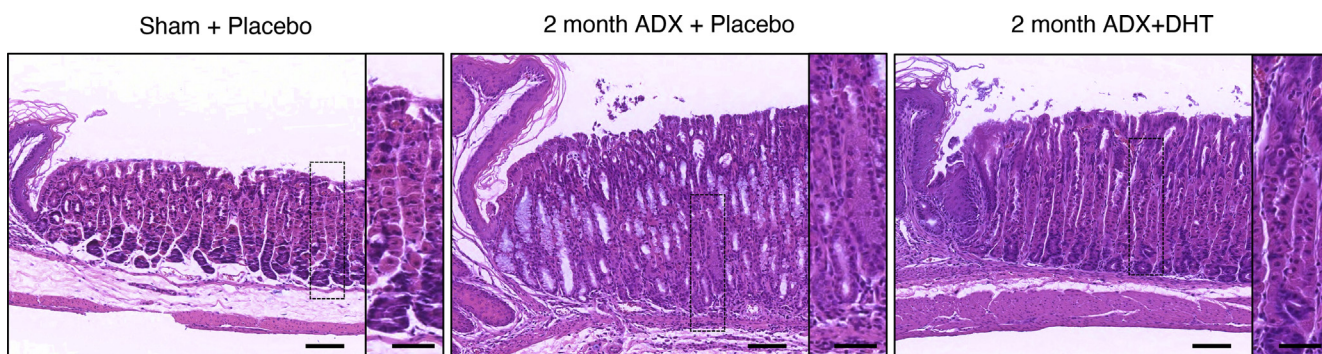
#### Transcript Profiling:

GSE147177.

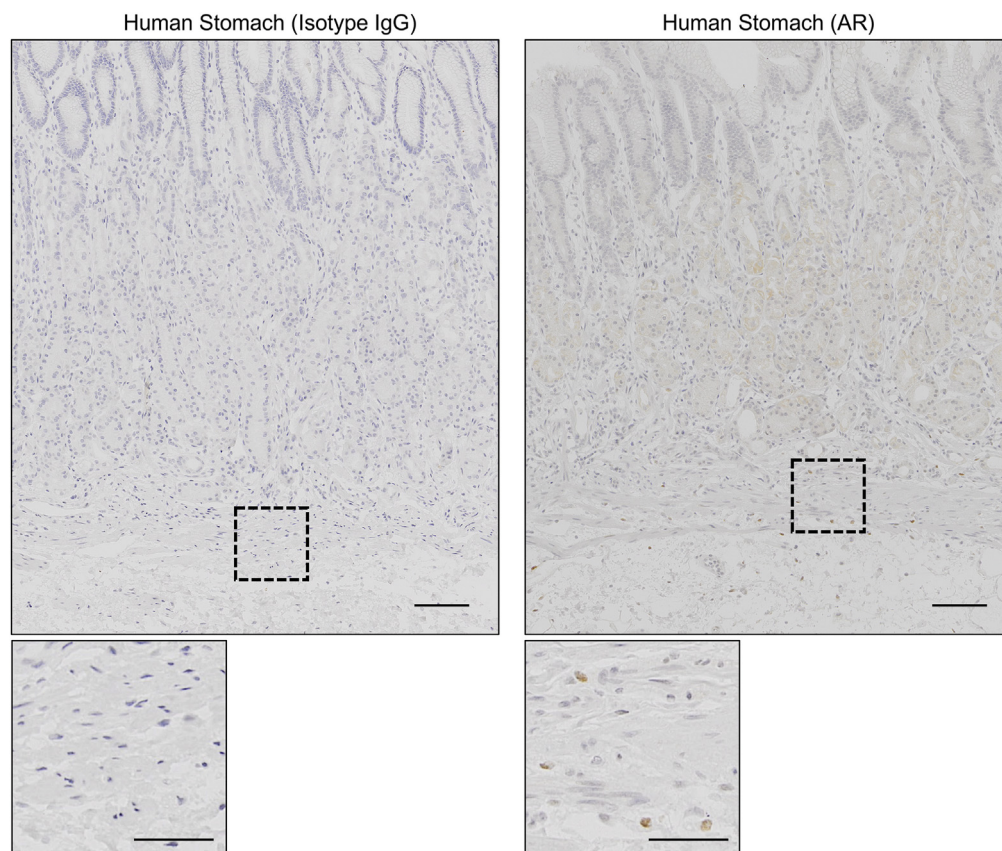




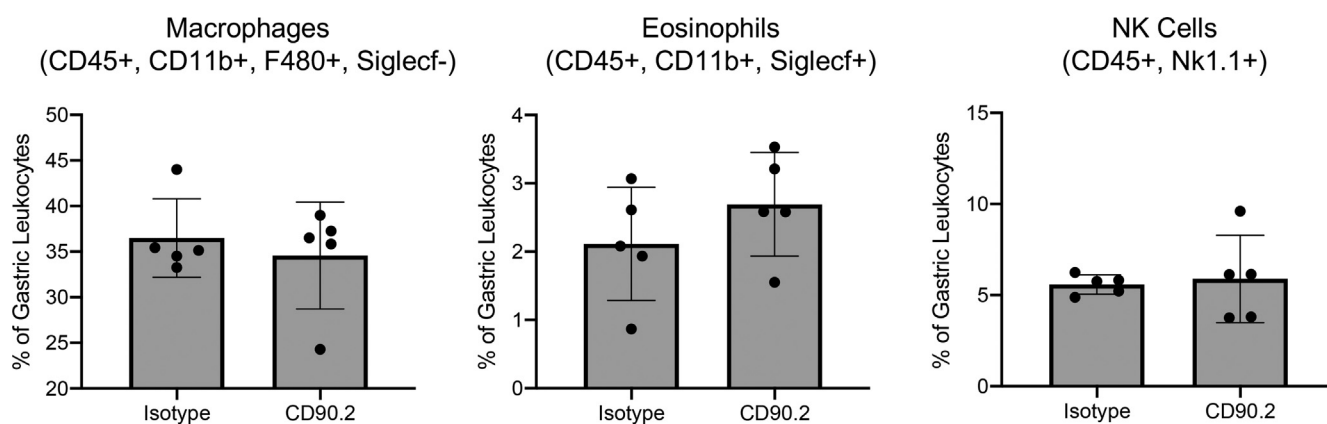
**Supplementary Figure 1.** Glucocorticoids are required to suppress gastric inflammation in females but are dispensable in males. (A) Schematic indicating the region of the gastric corpus used for analysis. (B) Representative immunostaining of stomach sections probed for CD45 (leukocytes, green). Nuclei are stained with DAPI. Scale bars are 100  $\mu$ m.  $n \geq 6$  mice/group.



**Supplementary Figure 2.** Androgens protect from ADX-induced SPEM. Representative H&E-stained micrographs of the gastric corpus from female mice that were simultaneously adrenalectomized and treated with DHT for 2 months.  $n \geq 5$  mice/group.

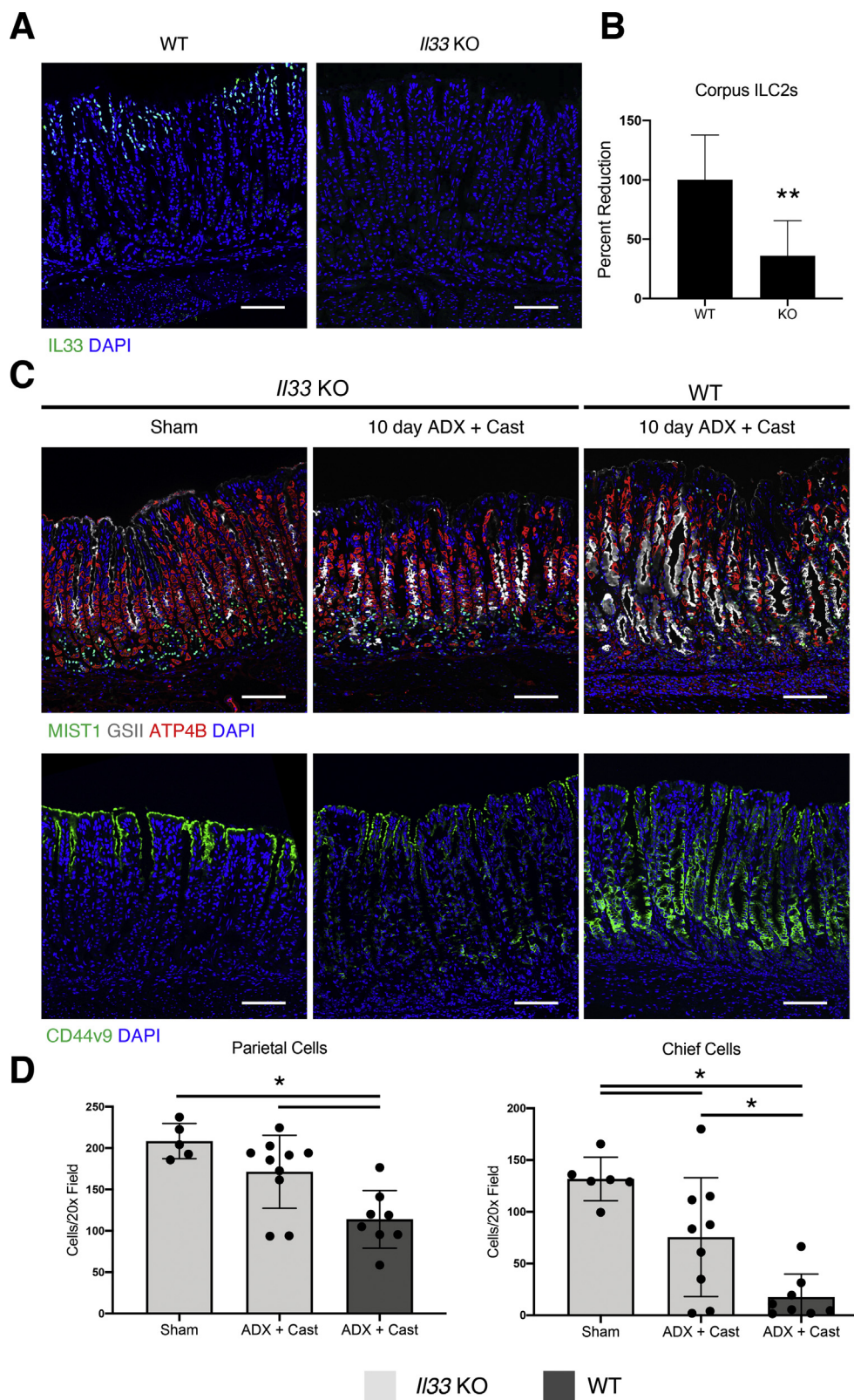


**Supplementary Figure 3.** AR expression in human stomach tissue closely reflects expression in the mouse. (A) Representative stomach sections from human tissue biopsies. Sections were probed with anti-AR antibodies or with isotype control antibodies. Scale bar = 100  $\mu\text{m}$  and 25  $\mu\text{m}$  in the inset.  $n = 8$ .



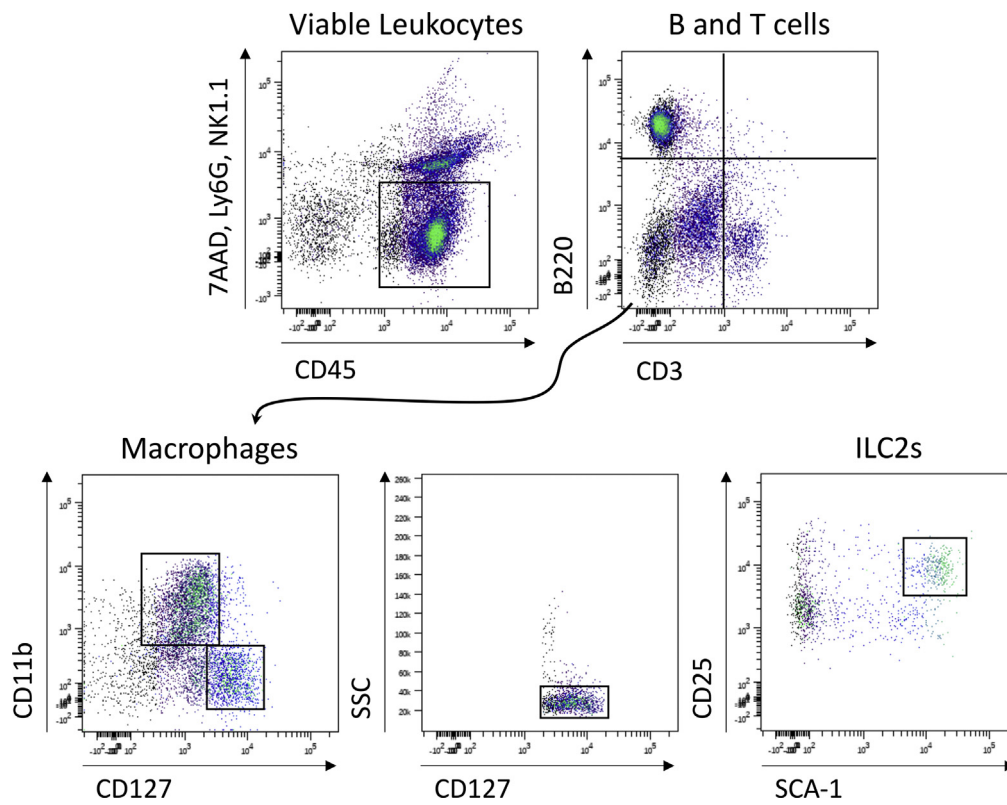
**Supplementary Figure 4.** ILC2 depletion does not change the stomach leukocyte composition. Flow cytometric analysis of the indicated cell populations from *Rag1* KO mice treated with CD90.2 or isotype control antibodies for 14 days. Data are mean  $\pm$  SD;  $P$ -values were determined using unpaired  $t$  test.  $n = 5$ .





**Supplementary Figure 5.** *Il33* KO mice are resistant to gastric inflammation and SPEM. (A) Immunostaining for IL33 in the gastric corpus of WT and *Il33* KO mice. (B) Percent reduction of ILC2s in the gastric corpus of WT and *Il33* KO mice. (C) Immunostaining of stomach sections taken from *Il33* KO and WT mice 10 days after surgery. Sections were probed for ATP4B (parietal cells, red), GSII lectin (mucous neck cells, white), and MIST1 (chief cells, green), or for CD44v9 (SPEM, green). Nuclei are stained with DAPI. Scale bars are 100  $\mu$ m. (D) Quantitation of the number of parietal cells and chief cells observed per 20x field ( $n \geq 5$  mice/group). All data are mean  $\pm$  SD;  $P$ -values were determined using 1-way analysis of variance with post hoc Tukey  $t$  test. \* $P \leq .05$ ; \*\* $P \leq .001$ .





**Supplementary Figure 6.** Gating strategy for the isolation of intestinal leukocyte populations. B cells were B220+, T cells were CD3+, macrophages were Ly6G-, NK1.1-, B200-, CD3- and CD11b+, and ILC2s were lineage-, SSC low, and CD127, CD25, and SCA-1+.